Journal of The Electrochemical Society, **150** (2) G83-G89 (2003)
0013-4651/2003/150(2)/G83/7/$7.00 © The Electrochemical Society, Inc.

Effects of Nitrogen Plasma Treatment on Tantalum Diffusion Barriers in Copper Metallization

Wen-Fa Wu,[a,*,z] Keng-Liang Ou,[b] Chang-Pin Chou,[b] and Chi-Chang Wu[a]

[a]*National Nano Device Laboratories, Hsinchu 300, Taiwan*
[b]*Institute and Department of Mechanical Engineering, National Chiao-Tung University, Hsinchu 300, Taiwan*

In this study, the barrier properties of ultrathin Ta, TaN, and nitrogen plasma-treated Ta films were investigated by Cu/Ta(N)/Si structure. The barrier properties were evaluated by sheet resistance, film stress, X-ray diffraction, transmission electron microscopy, scanning electron microscopy, atomic force microscopy, and X-ray photoelectron spectroscopy. Nitrogen plasma-treated Ta films possess better barrier performance than sputtered Ta and TaN films. The sheet resistance of Cu/Ta/Si and Cu/TaN/Si increases, apparently, after annealing at 600 and 625°C, respectively. The Cu/30 min plasma-treated Ta/Si is fairly stable up to annealing at 700°C for 1 h. Diffusion resistance of the plasma-treated Ta barrier is more effective. It is believed that a new amorphous layer forms on the surface of Ta film after plasma treatment. The new amorphous layer possesses some nanocrystalline Ta_2N phases with lattice constant 0.305 nm. It is believed that the amorphous layer containing some nanocrystals can alleviate Cu diffusion into the Si substrate and, hence, improve barrier performance.
© 2003 The Electrochemical Society. [DOI: 10.1149/1.1531974] All rights reserved.

Manuscript submitted October 1, 2001; revised manuscript received May 28, 2002. Available electronically January 2, 2003.

Copper is an attractive material for interconnection due to its lower electrical resistivity and better electromigration resistance compared to Al-based alloys. Copper is better considered for application in integrated circuits. However, it is well known that copper diffuses quickly in Si substrates and SiO_2 films, which causes degradation of transistor reliability by forming particular impurity levels in the silicon.[1] Because of its ability to rapidly diffuse in silicon and degrade reliability, the development of effective diffusion barrier materials is the most important issue for the realization of Cu interconnection in Si-based integrated circuits. Many materials are used as diffusion barriers in copper metallization system. Refractory metals and their nitrides have been investigated for such applications. Among them, tantalum and tantalum nitride have received the most attention owing to their high thermal stability and resistance to form compounds with copper. Previous studies have shown that tantalum nitride is more desirable than tantalum in terms of barrier effectiveness. However, resistivity of tantalum nitride film is higher than that of tantalum film.[2-4] As the technology moves to 180 nm node and below, a thin barrier layer is necessary to lower the resistance of the total line interconnect and/or via. It becomes inappropriate to use a barrier layer thicker than 30 nm, and hence investigations of the thermal stability and barrier properties of ultrathin barrier layers in the Cu metallization system are important.

In this article, we studied the barrier properties and thermal stability of ultrathin Ta-based barrier layers (10 nm) in the Cu metallization system. Furthermore, a new method to form nitrogen incorporated Ta film with low resistivity and high thermal stability was proposed and investigated. Nitrogen plasma was used to post-treat the Ta diffusion barrier. Properties of barrier layers were evaluated by electrical measurements and material analyses.

Experimental

The substrates used in these experiments were p-type (100) oriented silicon wafers with resistivity of 5-10 Ω cm. The Si wafers were cleaned in a dilute HF solution ($HF:H_2O = 1:20$) for 2 min, and rinsed in deionized (DI) water prior to loading into the sputtering system. The 10 nm Ta films were deposited at a power of 500 W and a sputtering pressure of 6.4 mTorr after the base pressure was evacuated to below 5×10^{-7} Torr. Some wafers further received *ex situ* nitrogen plasma treatments in a plasma enhanced chemical vapor deposition (PECVD) system after tantalum films were deposited. In addition, 10 nm tantalum nitride films were also deposited by reactive sputtering for comparison. The tantalum nitride films were prepared using optimum conditions as in our previous investigations, and thus provided a more effective barrier against Cu diffusion.[2] For easy identification, the sputtered tantalum, tantalum nitride, and nitrogen plasma-treated tantalum films were denoted as Ta, TaN, and TaN_x/Ta. Copper films, 300 nm thick, were deposited on top of the barrier layers. Cu/Ta/Si, Cu/TaN/Si, and Cu/TaN_x/Ta/Si were annealed in N_2 ambient from 500 to 800°C for 1 h to evaluate the thermal stability.

To realize the properties of Ta-based barrier layers, they were analyzed by atomic force microscopy (AFM), sheet resistance, and film stress. The film stress was obtained by measuring the changes in the radius of curvature of the substrate using laser scanning technology. In addition, X-ray photoelectron spectroscopy (XPS) using monochromatized Mg Kα radiation was performed to identify the chemical states of tantalum films with N_2 plasma treatments. To realize the capability of barrier layer against copper diffusion, the microstructure was observed using transmission electron microscopy (TEM). Surface morphology of annealed Cu/barrier/Si was observed by scanning electron microscopy (SEM). Compositions of failure sites were analyzed by energy-dispersive spectrometry (EDS) after removing both copper and barrier layers with a wet chemical solution. Grazing incidence X-ray diffractometry (GIXRD) was car-

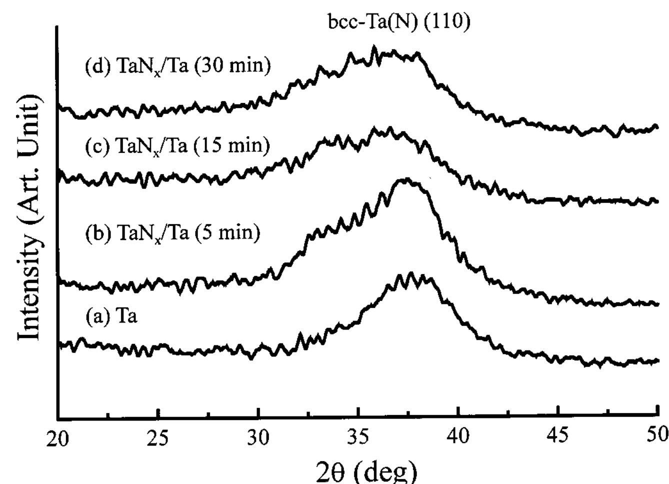

Figure 1. XRD spectra of sputtered and nitrogen plasma-treated Ta (10 nm) films.

* Electrochemical Society Active Member.
z E-mail: wfwu@ndl.gov.tw

Downloaded on 2014-04-27 to IP 140.113.38.11 address. Redistribution subject to ECS terms of use (see ecsdl.org/site/terms_use) unless CC License in place (see abstract).

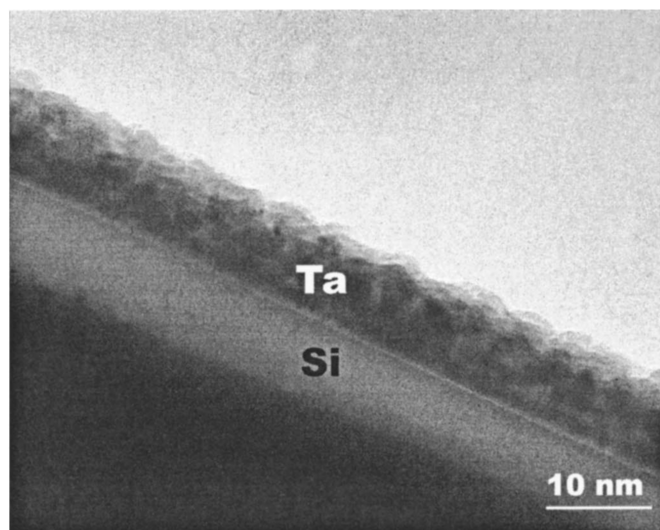

(a)

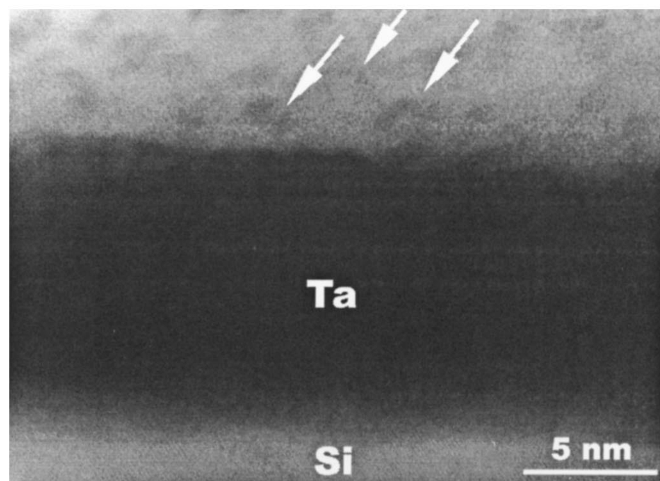

(b)

Figure 2. (a) Cross-sectional TEM micrograph of 30 min plasma-treated Ta (10 nm)/Si. (b) Corresponding high resolution TEM micrograph.

ried out for phase identification. The incident angle of the X-ray was fixed at 3°. Cu/barrier/n^+-p junction diodes with conventional localized oxidation of silicon (LOCOS) isolation were fabricated for electrical analyses. Leakage currents of the diodes were measured by HP4145B semiconductor parameter analyzer at a reverse bias of −5 V. After annealing at various temperatures for 1 h, the diode leakage current was measured.

Results and Discussion

Properties of N_2 *plasma-treated Ta films.*—Figure 1 shows the X-ray diffraction (XRD) spectra of 10 nm Ta films with and without plasma treatments. The time shown in the parenthesis is the period of the nitrogen plasma treatment. The intensity and shape of reflection indicate changes in the phase of the Ta film. By XRD analyses, it is obvious that as plasma-treatment time increases, the peak shape of body-centered cubic (bcc)-Ta(N)(110) phase becomes broad gradually. The phenomenon indicates lattice distortion and/or development of an amorphous Ta(N) thin film after plasma treatment. Figure 2 shows cross-sectional TEM micrographs of 30 min plasma-treated Ta/Si. The development of an amorphous TaN_x layer on the film surface was observed after the plasma treatment. The thin amor-

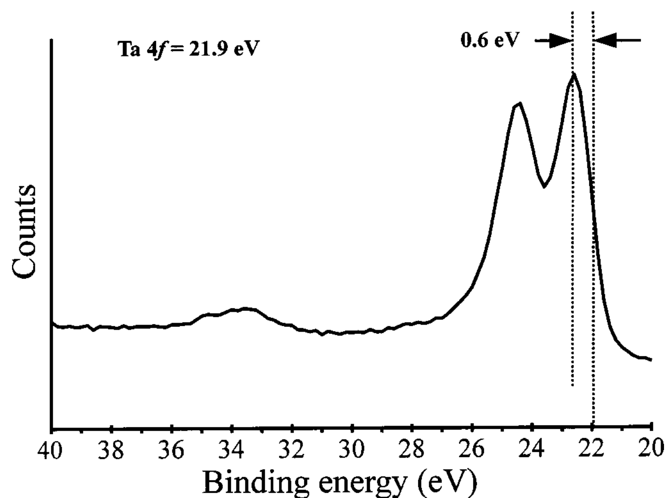

Figure 3. Ta 4f XPS spectrum obtained from the Ta film with nitrogen plasma treatment of 5 min.

phous layer possesses some nanocrystalline Ta_2N phases (denoted by arrows) with lattice constant 0.305 nm, as shown in Fig. 2b. Chemical bonding states of Ta films with N_2 plasma treatments were analyzed by XPS. Figure 3 shows the Ta 4f spectrum of the Ta film with the N_2 plasma treatment for 5 min. In compared with the Ta 4f peak of metal tantalum in the Handbook of X-Ray Photoelectron Spectroscopy,[5] 5 min plasma-treated Ta film [denoted as TaN_x/Ta (5 min)] indicates a chemical shift of 0.6 eV. It is attributed to the formation of Ta-N bond, which corresponds well to the value of the chemical shift reported as Ta_2N in the article.[6] It reveals that the chemical state of Ta_2N compound forms after the N_2 plasma treatment. Figure 4 shows the N 1s spectra of Ta films with various plasma-treatment time. It can give information concerning nitridation effects. Significant changes in N 1s peak are observed for Ta films with various plasma-treatment time. With N_2 plasma treatments, one peak at ~398 eV is found in the N 1s spectrum. It is attributed to $N^{\delta-}$, which is similar to the nitride ion.[7,8] The presence of the N 1s peak in Fig. 4 shows clearly that the surface is nitrided by nitrogen plasma. As the N_2 plasma treatment time increased to 30 min, another N 1s peak at ~401 eV is found in the N 1s spectrum. The peak at ~401 eV is ascribed to the nitrogen atoms or molecules

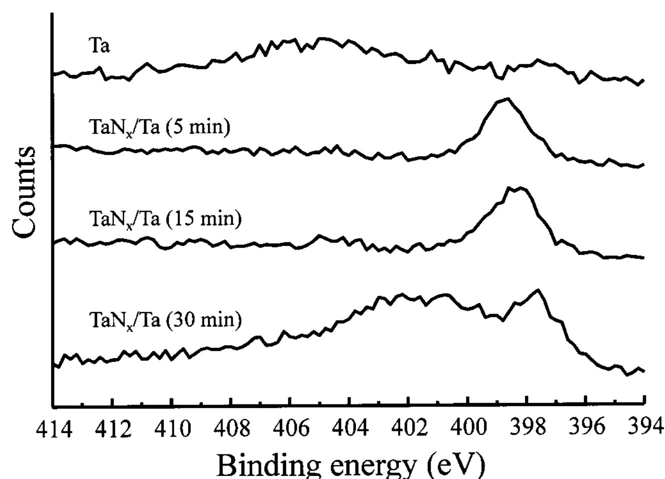

Figure 4. N 1s XPS spectra obtained from the Ta films with nitrogen plasma treatments for various plasma treatment times.

Downloaded on 2014-04-27 to IP 140.113.38.11 address. Redistribution subject to ECS terms of use (see ecsdl.org/site/terms_use) unless CC License in place (see abstract).

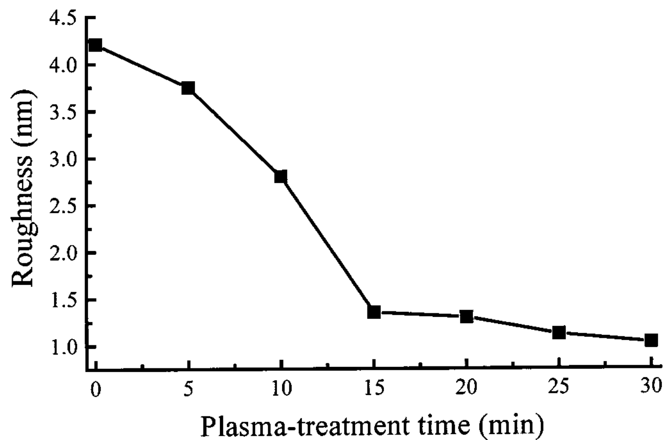

Figure 5. RMS surface roughness of Ta thin film as a function of plasma-treatment time.

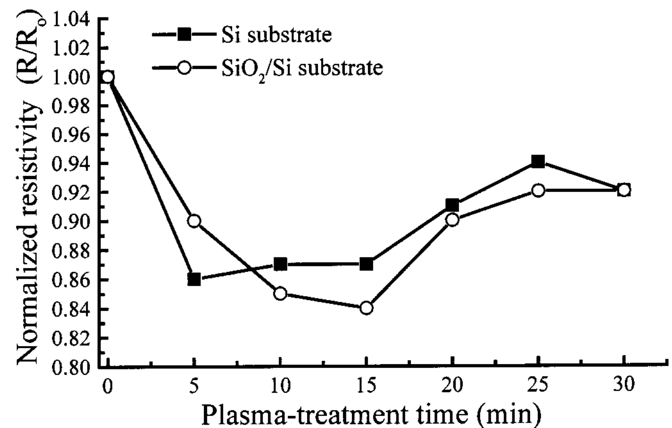

Figure 7. Normalized resistivity of TaN_x/Ta as a function of plasma-treatment time.

present in interstitial sites. This kind of nitrogen is also detected in tungsten films prepared by the reduction of WF_6 with N_2 in nitrogen gas.[8] These results indicate that some N atoms do not form strong covalent or ionic bonds with Ta atoms during the plasma nitridation of Ta film. Some of the introduced N atoms segregate at the interstitial sites and grain boundaries in the tantalum film as impurities. Similar results were reported for plasma nitridation of chemical vapor deposited (CVD) tungsten by Chang *et al.*[7] This result is consistent with high-resolution (HR) TEM observation. As the plasma-treatment time increases, the amorphous layer with Ta_2N nanoparticles embedded inside was formed. Figure 5 shows root-mean-square (rms) surface roughness as a function of plasma-treatment time. The surface roughness is measured by AFM. It can be seen that the longer the plasma-treatment time, the smoother the surface. The surface roughness of as-sputtered Ta and TaN_x/Ta (30 min) films are 4.21 and 1.08 nm, respectively. It is believed that sputtering and/or stuffing effects would occur due to the reactions or bombardments of energetic radicals and ions during plasma treatment. They could sputter the films and make them smooth. Nitridation effects also occur during nitrogen plasma treatment. Chemical compositions of plasma-treated tantalum films were analyzed by XPS. It is found that nitrogen content increases with increasing plasma-treatment time. Nitrogen content of the Ta film with 5 min plasma treatment is 5.64 atom %. With plasma treatment for 30 min, nitrogen content is 32.12 atom %. Figure 6 shows stress of TaN_x/Ta barrier as a function of plasma-treatment time. After N_2 plasma treatment for 5 min, a high compressive stress developed in the TaN_x/Ta barrier. The stress transforms from compressive to tensile for films with N_2 plasma treatments longer than 15 min. The compressive stress could result from the lattice distortion, produced by incorporation of nitrogen atoms of a size different from the Ta film, and reaction and stuffing at grain boundaries. Atomic peening effect would induce compressive stress in plasma process. However, with further increase in the period of the nitrogen plasma treatment, amorphous films were formed and the stress becomes tensile. Figure 7 shows normalized resistivity of Ta films before and after plasma treatments.

The normalized resistivity is designated as the ratio of R to R_o (R/R_o), where R_o and R denote the resistivity of as-sputtered and plasma-treated Ta films, respectively. The resistivity of as-deposited Ta film is 197 $\mu\Omega$ cm. As plasma-treatment time increased from 5 to 15 min, the resistivity decreased initially and then increased. However, resistivity of 30 min plasma-treated Ta film does not increase further. In our previous study, it is found that resistivity of the reactively sputtered TaN film would initially decrease to 159 $\mu\Omega$ cm and then increase to higher than 3500 $\mu\Omega$ cm as nitrogen flow ratio increases during reactive sputtering.[2] Min *et al.* reported similar results. It is found that small nitrogen incorporation could result in the decrease of the resistivity of reactively sputtered Ta(N) film.[9] The formation of the amorphous layer would increase the resistivity due to increasing scattering effects. The variation in resistivity is due to the combined effects as mentioned above. The nitrogen incorpora-

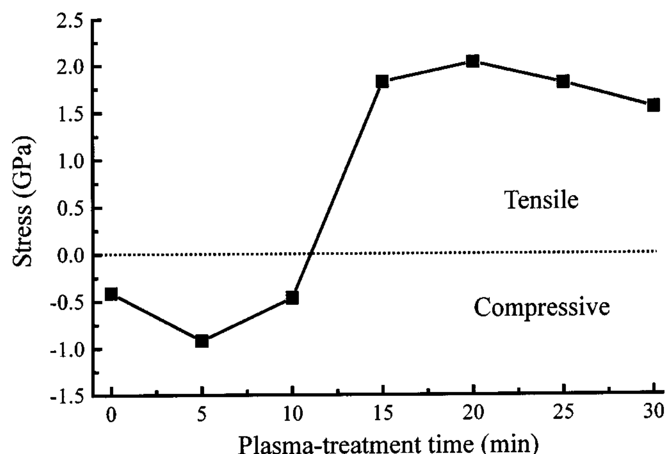

Figure 6. Stress of plasma-treated Ta/Si as a function of plasma-treatment time.

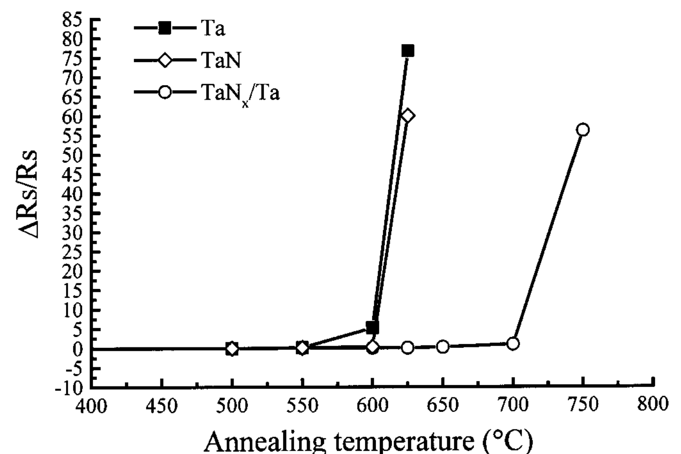

Figure 8. Variation in sheet resistance of Cu/Ta(N)/Si as a function of annealing temperature.

Downloaded on 2014-04-27 to IP 140.113.38.11 address. Redistribution subject to ECS terms of use (see ecsdl.org/site/terms_use) unless CC License in place (see abstract).

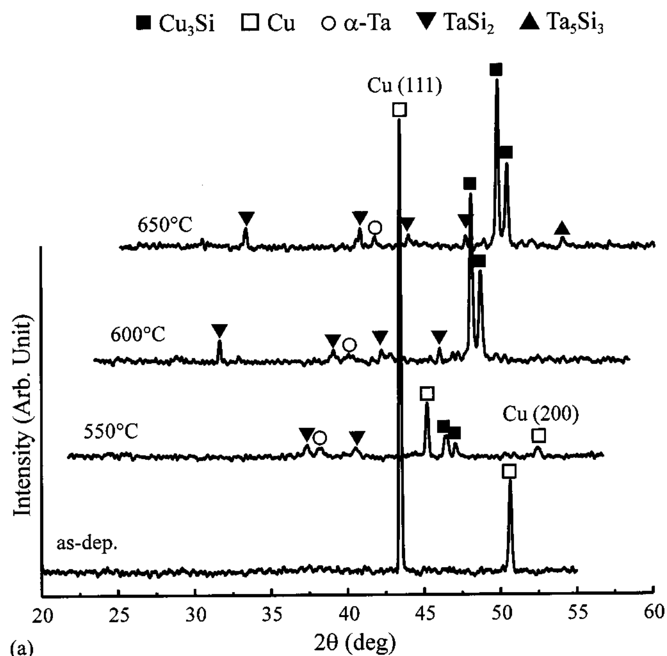

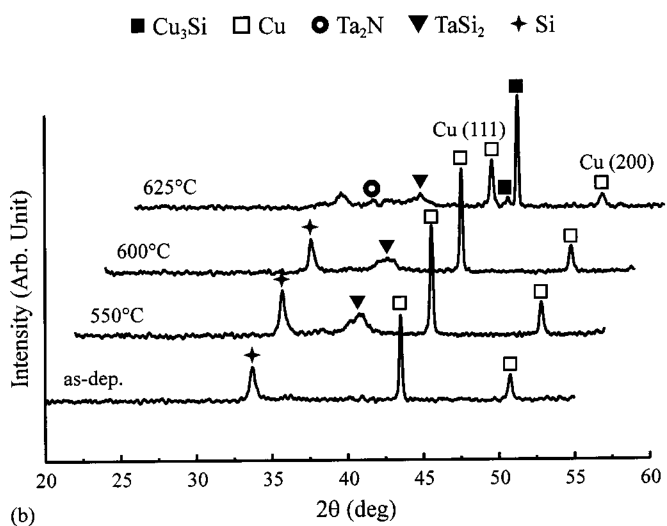

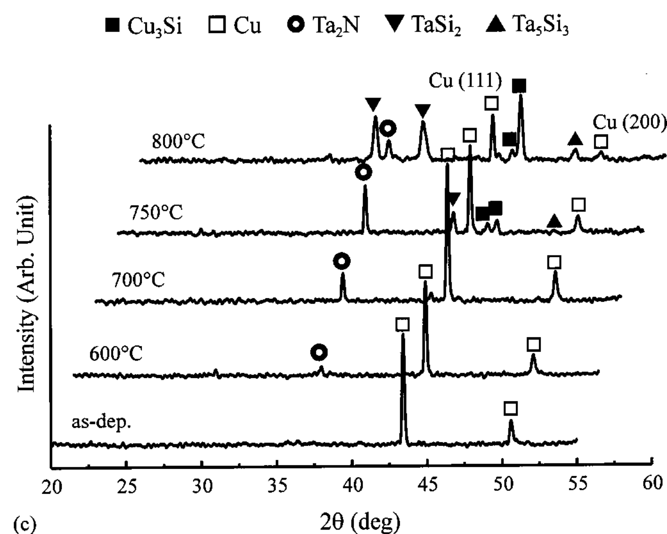

Figure 9. XRD spectra for (a) Cu/Ta/Si, (b) Cu/TaN/Si, and (c) Cu/TaN_x/Ta/Si after annealing at various temperatures.

Table I. XRD results of annealed Cu/barrier/Si.

Barrier layer	T_f^a (°C)	XRD results: $T < T_f$ (°C)	XRD results: T_f (°C)
Ta	600	α-Ta + Cu_3Si + Cu	Cu_3Si + tantalum silicide ($TaSi_2$) + α-Ta
TaN	625	$TaSi_2$ + $TaSi_2$ + Cu	Cu_3Si + tantalum silicide ($TaSi_2$) + Cu
TaN_x/Ta (30 min)	750	Ta_2N + $TaSi_2$ + Cu	Cu_3Si + tantalum silicide ($TaSi_2$ and Ta_5Si_3) + Cu + Ta_2N

[a] T_f is failure temperature.

tion is the dominant factor in the early plasma treatment. Resistivity would increase due to the development of the amorphous layer after increasing plasma treatment.

Thermal stability of Cu/Ta(N)/Si.—Figure 8 shows the variation in sheet resistance of Cu/Ta(N)/Si as a function of annealing temperature. The data mainly indicates changes in the thickness or resistivity of the unreacted copper layer, since the resistance of the barrier layer and reaction products are expected to be much larger than that of Cu. It is found that sheet resistance of annealed Cu/barrier/Si is slightly lower than that of as-deposited after low temperature annealing. It is acribed to a decrease in defect density and grain growth of Cu film.[1] Low sheet resistance is obtained for all samples before they are annealed at the failure temperature. In the study, the failure temperature is defined as the temperature that the great increase of sheet resistance is found after annealing. As shown in Fig. 8, the sheet resistance of Cu/Ta/Si increases greatly after annealing at 600°C. Moreover, a change in color of copper surface and production of precipitate are found. It reveals that significant reactions have occurred between the layers. The increase of sheet resistance may also result from agglomeration of copper film after annealing. No obvious change in sheet resistance was observed for Cu/TaN/Si at the annealing temperature of 600°C. However, great increase is also found after annealing at 625°C. Cu/TaN_x/Ta/Si remains low sheet resistance even after annealing at 700°C for 1 h. It is obvious that an N_2 plasma-treated Ta (TaN_x/Ta) barrier layer possesses higher thermal stability than Ta and TaN barrier layers. XRD analyses are performed to identify the phase formation of the Cu/Ta(N)/Si samples after high temperature annealing. Figure 9 illustrates the XRD spectra for Cu/Ta/Si, Cu/TaN/Si, and Cu/TaN_x/Ta/Si samples subjected to anneal at various temperatures. Strong Cu(111), and weak Cu(200) peaks are observed in as-deposited and annealed samples, indicating that the Cu films have preferred ⟨111⟩ crystal orientation. It has been reported that Cu with high ⟨111⟩ texture provides higher electromigration resistance.[10] For the Cu/Ta/Si sample annealed at 550°C, signals of $TaSi_2$ and Cu_3Si phases are detected. After annealing at 600°C, the signal of Cu disappeared while peaks of Cu_3Si increase obviously, indicating the failure of the Ta barrier layer. The high resistivity Cu_3Si formation and related Cu decrease resulted in the great increase of sheet resistance as shown in Fig. 8. For the sample with the TaN barrier layer, a Cu_3Si phase was detected after annealing at 625°C. In contrast to Cu/Ta/Si, peaks of Cu were still observed after annealing at 625°C for 1 h. Clearly, thermal stability of the Cu/TaN/Si is superior to that of the Cu/Ta/Si contact system. XRD results of Cu/TaN_x/Ta/Si samples show that the crystallization of the amorphous-like TaN_x layer occurs after annealing at 600°C. As shown in Fig. 9c, Ta_2N and $TaSi_2$ phases were detected after annealing at 600 and 700°C, respectively. After annealing at 750°C for 1 h, peaks of Cu_3Si are detected. In respect of the phase formation of tantalum silicide, the formation temperature of the sample with TaN_x/Ta barrier was

Downloaded on 2014-04-27 to IP 140.113.38.11 address. Redistribution subject to ECS terms of use (see ecsdl.org/site/terms_use) unless CC License in place (see abstract).

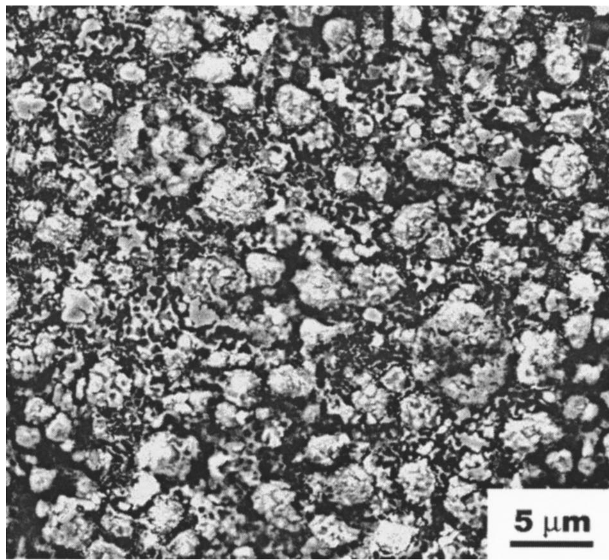

(a)

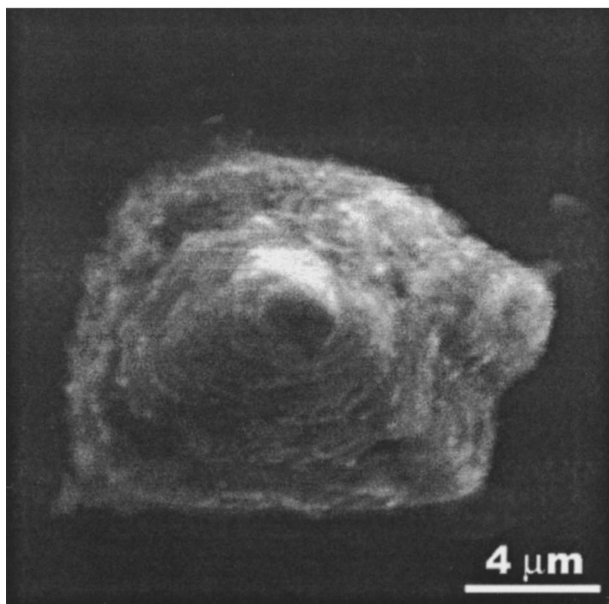

(b)

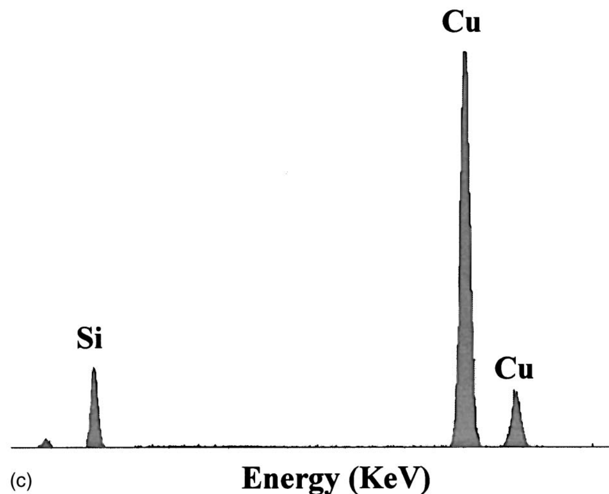

(c)

Figure 10. (a) SEM micrograph of Cu/Ta(N)/Si sample annealed at failure temperature. (b) Enlarged image of the precipitate. (c) EDS spectrum obtained from the precipitate.

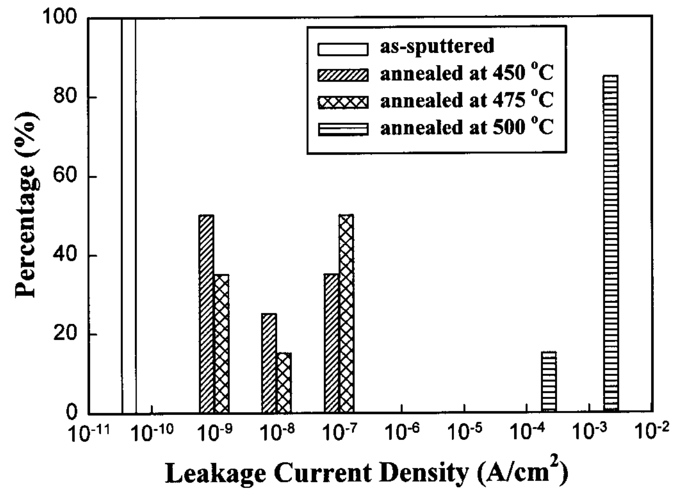

(a)

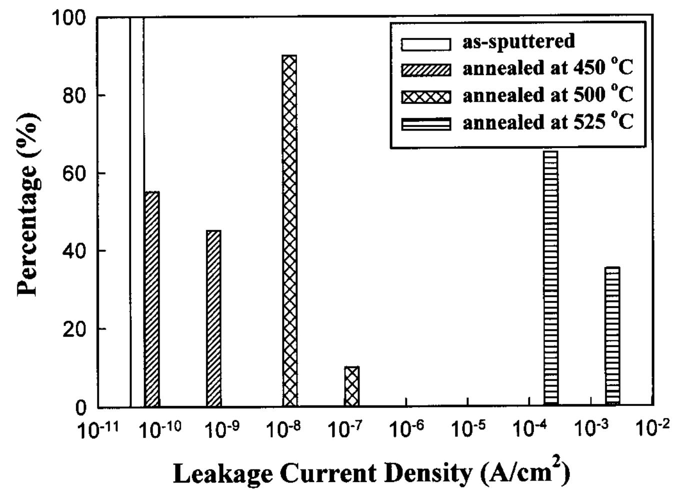

(b)

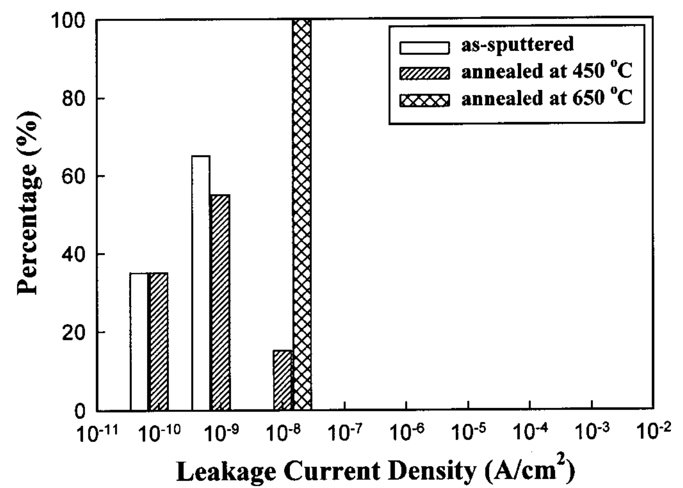

(c)

Figure 11. Distributions of leakage current density of the (a) Cu/Ta/Si, (b) Cu/TaN/Si, and (c) $Cu/TaN_x/Ta/Si$ n^+-p junction diodes after annealing at various temperatures for 1 h.

Downloaded on 2014-04-27 to IP 140.113.38.11 address. Redistribution subject to ECS terms of use (see ecsdl.org/site/terms_use) unless CC License in place (see abstract).

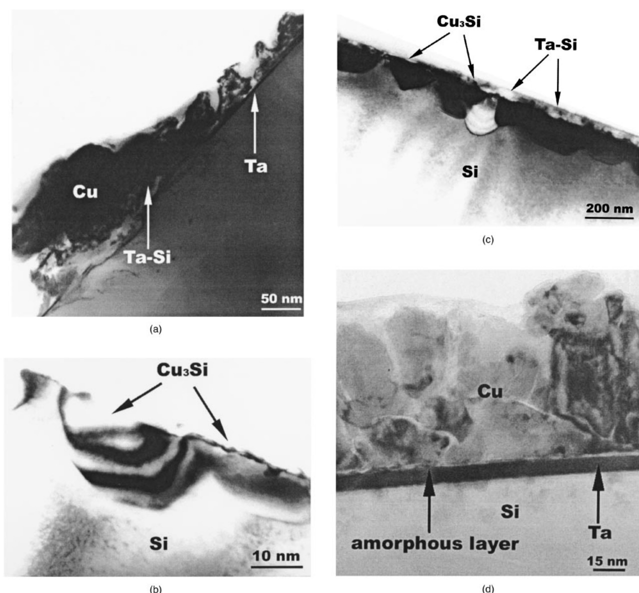

Figure 12. Cross-sectional TEM micrographs of (a) 550°C-annealed Cu/Ta/Si, (b) Cu_3Si precipitates, (c) 625°C-annealed Cu/TaN/Si, and (d) 600°C-annealed Cu/TaN_x/Ta/Si.

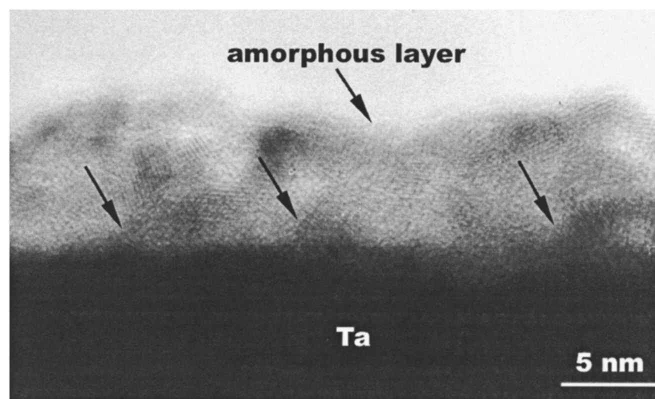

Figure 13. HRTEM micrograph of Cu/TaN_x/Ta interface in Cu/TaN_x/Ta/Si sample after annealing at 600°C for 1 h.

higher than that of the sample with Ta or TaN barrier. That is, nitrogen plasma treatment will restrain formation of tantalum silicide, attributed to formation of a nanostructured amorphous barrier layer to alleviate Cu diffusion. It was reported that Cu penetration would promote Ta silicide formation.[11] Table I summarizes XRD results of Cu/Ta/Si, Cu/TaN/Si, and Cu/TaN_x/Ta/Si after annealing at various temperatures for 1 h. The failure temperatures of Ta, TaN, and TaN_x/Ta barrier layers are 600, 625, and 750°C, respectively. It is found that phases of copper silicide and tantalum silicide were detected after annealing at the failure temperature. For further analysis of the thermal stability, SEM was used to examine the surface morphologies of Cu films after thermal annealing. After annealing at the temperature higher than the failure temperature, protrusions or precipitates were observed on the surface. Figure 10 shows the typical SEM micrographs of Cu/barrier/Si after annealing at the temperature higher than the failure temperature. As shown in Fig. 10a, protrusions are observed on the surface, indicating a severe reaction of Cu/barrier/Si. Figures 10b and c show enlarged image of the protrusion and corresponding EDS spectrum. It reveals that the protrusion consisted of elemental Cu and Si, and was a copper-rich region. These protrusions are presumably caused by Cu diffusion through the localized weak point in the barrier and reacting with underlying Si to form Cu_3Si. Similar phenomena were reported for Ta diffusion barriers by Hollway *et al.*[11] Barrier capabilities of ultrathin Ta, TaN, and TaN_x/Ta films are further investigated by evaluating the thermal stability of Cu/barrier/n^+-p junction diodes using electrical measurements. Figure 11 illustrates the statistical distributions of reverse biased leakage current densities for Cu/barrier (10 nm)/n^+-p junction diodes annealed at various temperatures. If we define a failure criterion with 10^{-6} A/cm^2, the Cu/Ta/n^+-p diodes remain stable after annealing at temperatures up to 475°C but suffered degradation at 500°C (Fig. 11a). It is reported that the barrier properties of Ta can be improved by adding impurities, such as N and O.[2,4,12] Figure 11b shows the statistical distributions of reverse biased leakage current densities for the Cu/TaN/n^+-p junction diodes annealed at various temperatures. For the diodes with 10 nm TaN barriers, the diodes remained stable after annealing at temperatures up to 500°C. After annealing at 525°C, failure of the diodes was observed. Tsai *et al.* reported similar results. It was found that the diodes with 60 nm CVD and physical vapor deposited TaN barriers would begin to deteriorate at 500 and 550°C, respectively.[12] It is shown that barrier capability of TaN film is better than that of Ta film. However, the improvement is limited. Furthermore, the resistivity of reactively sputtered TaN will increase significantly with increasing nitrogen concentration. The resistivity of the TaN film sputtered at 35% nitrogen flow ratio would increase to ~3500 μΩ cm, from ~190 μΩ cm for the Ta film.[2] As mentioned previously, nitrogen incorporated

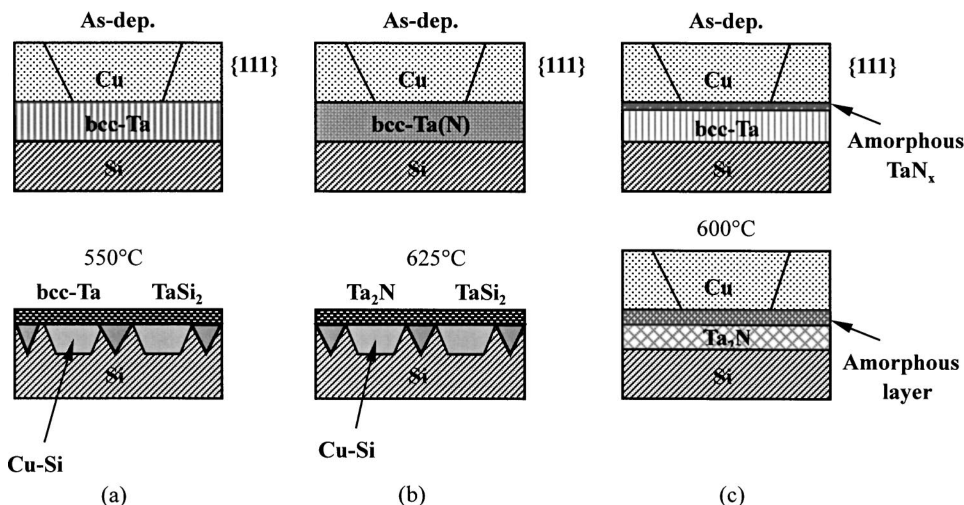

Figure 14. Schematic illustrations of the microstructures of (a) Cu/Ta/Si (b) Cu/TaN/Si, and (c) Cu/TaN_x/Ta/Si samples before and after annealing.

Downloaded on 2014-04-27 to IP 140.113.38.11 address. Redistribution subject to ECS terms of use (see ecsdl.org/site/terms_use) unless CC License in place (see abstract).

Ta films (TaN_x/Ta) were also prepared by nitrogen plasma treatment in the study. The resistivity of TaN_x/Ta was as low as that of as-sputtered Ta, as shown in Fig. 7. The $Cu/TaN_x/Ta/n^+$-p diodes retained electrical integrity even after annealing at 650°C, as shown in Fig. 11c. The TaN_x/Ta films possess much better barrier performance than Ta and TaN films. The improved barrier performance is attributed to nanocrystallization and stuffing effects due to the reactions or bombardments of energetic radicals and ions during plasma treatment. It is reported that the microstructure within the barrier layer strongly affects the barrier performance because Cu diffuses through fast diffusion paths such as grain boundaries within the barrier layer.[2,9,13] The thin nanocrystalline TaN_x layer was formed on the surface of the Ta film after nitrogen plasma treatment, as shown in Fig. 2. A Nanostructured diffusion barrier is more effective for preventing Cu diffusion than a polycrystalline barrier because the nanostructured film does not have large-angle grain boundaries where most of the atomic diffusion typically occurs.[14]

Failure mechanism of Cu/Ta(N)/Si.—It is obvious that there exists the difference of failure mechanism among Ta, TaN, and TaN_x/Ta barriers as shown in the results of sheet resistance measurements and XRD analyses. Figure 12 shows cross-sectional TEM micrographs of annealed Cu/Ta/Si, Cu/TaN/Si, and $Cu/TaN_x/Ta/Si$. As shown in Fig. 12a, it is obvious that Ta silicide and Cu silicide were observed after annealing, and the interface of the sample is not clear. It indicates the degradation of the Ta barrier after annealing at 550°C for 1 h. The as-deposited Ta film consists of fine ($\sim$20 nm) columnar grains. The degradation of the Ta barrier is attributed to the diffusion of Cu into the Si substrate through the columnar Ta barrier. Figure 12b illustrates the corresponding image of the Cu_3Si precipitate in the Si substrate. Trapezoidal-shaped copper silicide spikes bounded by Si{111} and Si{001} planes are observed.[11] Figure 12c shows the TEM image of the Cu/TaN/Si sample after annealing at 625°C for 1 h. The multilayered structure is destroyed and triangular and trapezoidal Cu_3Si precipitates form with the disappearance of Cu overlay. It indicates degradation of the TaN barrier at 625°C. Figure 12d shows the TEM image of $Cu/TaN_x/Ta/Si$ sample after annealing at 600°C for 1 h. There exists an amorphous layer between the Cu and Ta-based barrier layers. Neither Cu silicide nor Ta silicide were observed at the interface, which shows the excellent barrier properties. The corresponding high resolution TEM image of annealed $Cu/TaN_x/Ta/Si$ sample, is shown in Fig. 13. It indicated that the nanocrystalline Ta_2N phase appears within the amorphous layer. Furthermore, microtwins (denoted as narrows) are found at Ta and Ta_2N interface.

Cross sections of the interfacial structures before and after annealing are shown schematically in Fig. 14a, b, and c for the Cu/Ta/Si, Cu/TaN/Si, and $Cu/TaN_x/Ta/Si$ samples, respectively. Cu films on Ta, TaN, and TaN_x/Ta barriers have preferred {111} orientation. The as-deposited Ta barrier has a Ta bcc structure with fine ($\sim$20 nm) columnar grains as shown in Fig. 14a. Formation of $TaSi_2$ and copper silicide were observed after annealing at 550°C for 1 h, indicating the barrier degradation. The mechanism by which the barrier fails is the motion of Cu through the columnar Ta to form Cu_3Si. The barrier capability of the Ta film against Cu diffusion can be improved by incorporating nitrogen in the Ta film using reactive sputtering. The structure of the reactively sputtered TaN films will change from voided columnar to fibrous and featureless with increasing nitrogen flow ratio, and the TaN film with amorphous-like structure functions as a more effective barrier against Cu diffusion.[2,15] The as-deposited TaN barrier has a Ta(N) bcc structure, as shown in Fig. 14b. No Cu silicide is observed for Cu/TaN/Si sample after annealing at 600°C for 1 h, indicating better barrier property than that of Ta. However, the barrier capability of the Ta film is improved moderately by incorporating nitrogen with reactive sputtering. Similar trapezoidal or triangular Cu_3Si precipitates formed with the disappearance of Cu overlay after annealing at 625°C for 1 h, as shown in Fig. 14b. The formation of a thin amorphous TaN_x layer on the surface of Ta film is observed after the nitrogen plasma treatment. The TaN_x/Ta barrier prevented the Cu/Si reaction as shown in Fig. 14c. There exists an amorphous layer between the Cu and barrier layers after annealing at 600°C for 1 h. The barrier retains its integrity and no Cu silicide or Ta silicides were observed. Nanocrystallization and stuffing effects of plasma treatments would alleviate the Cu diffusion and hence enhance barrier stability. High thermal stability of $Cu/TaN_x/Ta/Si$ is obtained.

Conclusion

Nitrogen incorporated Ta films (TaN_x/Ta) were prepared by nitrogen plasma treatment. The resistivity of TaN_x/Ta was as low as that of as-sputtered Ta film. Barrier properties of TaN_x/Ta are better than those of sputtered Ta and TaN. As plasma-treatment time increases, the surface roughness decreases obviously. Nanocrystallization and stuffing effects as well as nitridation were observed. With the reactions and bombardments of nitrogen ions and radicals, a new amorphous layer induces on the surface of the Ta barrier. The barrier stability of the Ta films enhanced apparently after nitrogen plasma treatment. The $Cu/TaN_x/Ta$ (10 nm)/Si remained stable after annealing at 700°C for 1 h. The failure temperature of TaN_x/Ta barrier is at least 150°C higher than that of the Ta barrier. Nanocrystallization and stuffing effects of plasma treatments are believed to impede Cu diffusion into the Si substrate and, hence, improve the barrier performance.

Acknowledgments

The authors would like to thank the National Science Council of Republic of China for financially supporting this research under contract no. NSC 90-2215-E-317-005 and NSC 91-2722-2317-200.

National Nano Devices Laboratories assisted in meeting the publication costs of this article.

References

1. Y. J. Lee, B. S. Suh, M. S. Kwon, and C. O. Park, *J. Appl. Phys.,* **85**, 1927 (1999).
2. W. L. Yang, W. F. Wu, D. G. Lin, C. C. Wu, and K. L. Ou, *Solid-State Electron.,* **45**, 149 (2001).
3. M. T. Wang, Y. C. Lin, and M. C. Chen, *J. Electrochem. Soc.,* **145**, 2538 (1998).
4. X. Sun, E. Kolawa, J. S. Chen, J. S. Reid, and M. A. Nicolet, *Thin Solid Films,* **236**, 347 (1993).
5. J. F. Moulder, W. F. Stickle, P. E. Sobol, and K. D. Bomben, *Handbook of X-Ray Photoelectron Spectroscopy*, p. 170, Physical Electronics, Inc., Eden Prairie, MN (1995).
6. O. Ibidumni, R. L. MaSaitis, R. L. Opila, A. J. Davenport, H. S. Isaacs, and J. A. Taylor, *Surf. Interface Anal.,* **20**, 559 (1993).
7. K. M. Chang, T. H. Yeh, I. C. Deng, and C. W. Shih, *J. Appl. Phys.,* **82**, 1469 (1997).
8. T. Nakajima, K. Watanable, and N. Watanabe, *J. Electrochem. Soc.,* **134**, 3175 (1987).
9. K. H. Min, K. C. Chun, and K. B. Kim, *J. Vac. Sci. Technol. B,* **14**, 3263 (1996).
10. Y. L. Chin, B. S. Chiou, and W. F. Wu, *Jpn. J. Appl. Phys., Part 1,* **39**, 6708 (2000).
11. K. Holloway, P. M. Fryer, C. Cabral, Jr., J. M. E. Harper, P. J. Bailey, and K. H. Kelleher, *J. Appl. Phys.,* **71**, 5433 (1992).
12. M. H. Tsai, S. C. Sun, C. E. Tsai, S. H. Chuang, and H. T. Chiu, *J. Appl. Phys.,* **79**, 6932 (1996).
13. G. S. Chen and S. T. Chen, *J. Appl. Phys.,* **87**, 8473 (2000).
14. D. J. Kim, Y. T. Kim, and J. W. Park, *J. Appl. Phys.,* **82**, 4847 (1997).
15. G. S. Chen, P. Y. Lee, and S. T. Chen, *Thin Solid Films,* **353**, 264 (1999).

Downloaded on 2014-04-27 to IP 140.113.38.11 address. Redistribution subject to ECS terms of use (see ecsdl.org/site/terms_use) unless CC License in place (see abstract).